Electronic Supplementary Material (ESI) for Inorganic Chemistry Frontiers.

Au depositing and Mg doping synergistically regulates In_2O_3 photocatalyst for promoting CO_2 reduction and CH_4 exclusive generation

Yanduo Liu[a,*], Jiadong Li[b,*], Xianglan Dong[a], Lina Dai[a], Enqi Zhang[a]

[a] School of Chemistry and Chemical Engineering, Harbin Normal University, Harbin150025, Heilongjiang, China. E-mail: liuyd0608@163.com

[b] School of New Energy, Ningbo University of Technology, Ningbo315336, Zhejiang, China. E-mail: lijd@nbut.edu.cn

***Corresponding Authors.**

E-mail addresses: liuyd0608@163.com (Yanduo Liu), lijd@nbut.edu.cn (Jiadong Li)

Characterization techniques

A Bruker D8 Advance diffractometer was used to analyze the X-ray powder diffraction (XRD) using Cu Kα radiation. A Model Shimadzu UV-2750 spectrophotometer was adopted to record the UV-vis diffuse reflectance spectrum (DRS) by using with $BaSO_4$ as a reference. Morphologies of samples were observed by using a scanning electron microscope (SEM, HitachiS-4800 instrument, Tokyo, Japan) and Transmission electron microscopy (TEM, JEOL JEM-2010EX instrument), operating at acceleration voltage of 15 kV and a 200 kV accelerating voltage, respectively. A self-built equipment was applied to detect the steady-state surface photovoltage spectroscopy (SS-SPS), equipped with a lock-in amplifier (SR830, USA) synchronized with a light chopper (SR540, USA). A Kratos-Axis Ultra DLD apparatus with an Al (mono) X-ray source was used to measure the X-ray photoelectron spectroscopy (XPS). All the XPS spectra were calibrated according to the C 1s peak at 284.8 eV. The electron paramagnetic resonance (EPR) measurements were carried out on a Bruker EMX plus model spectrometer operating at the X-band frequency. The near ambient pressure (NAP)-XPS spectra were collected at the SPECS NAP-XPS. The light irradiation was introduced into the analysis chamber through an observation window using a 300 W xenon lamp.

Photoelectrochemical measurement

Using a conventional electrochemical workstation that had a standard three-electrode electro-chemical system tested the photoelectrochemical measurements (CHI760E, Shanghai). The film electrode was fabricated as follows: 50 mg of photocatalyst and 35 mL of terpineol were stirred vigorously to prepare the

experimental electrode. Then, the mixture was coated onto the FTO electrode and then calcined at 200 °C for 120 min. The working electrode, Pt plate and Ag/AgCl electrode were taken as the working electrode, the counter electrode and the reference electrode on a LK2006 A workstation, respectively. 1 M KOH solution was used as electrolyte and a 300W Xenon lamp (wavelength range: 320-780 nm, spot diameter: 60 mm, light power: 134 mW/cm^2) with a 420 nm cut off filter was used as light source. Mott-Schottky tests were conducted at frequencies of 500, 1000 and 1500 Hz.

Hydroxyl radical amount measurement

0.05 g of the sample was dispersed in 60 mL of 1×10^{-3} mol L^{-1} aqueous solution in a quartz reactor. The suspension was stirred for 30 min before irradiation. After a given irradiation time with a spectrofluorometer (PerkinElmer LS 55), a certain amount of the solution was transferred into a Pyrex glass cell for the fluorescence measurement of 7-hydroxycoumarin with characteristic emission peak at about 460 nm under the light excitation of 332 nm.

Evaluation for CO_2 temperature programmed desorption

CO_2-temperature programmed desorption (CO_2-TPD) were performed by Chemisorption Analyzer, TP 5080 Chemisorb with a thermal conductivity detector (TCD). 50 mg sample was preheated at 300 °C for 0.5 h to remove the other adsorbed gases and water and then cooled down to 30 °C under He flow rate of 30 mL min^{-1}. The pure CO_2 gas was introduced at 30 °C under CO_2 flow rate of 50 mL min^{-1} for 0.5 h. The excess weak physically adsorbed O_2 was removed by He flow rate of 30 mL min^{-1} at 30 °C for 60 min. Then the temperature was increased to 400 °C with the heating rate of 10 °C min^{-1} under He flow rate of 30 mL min^{-1}.

In situ DRIFTS measurements

The in situ diffuse reflectance infrared Fourier transform spectroscopy (DRIFTS)

analysis was carried out in an in situ diffuse reflectance pool with a Bruker Vector FTIR spectrometer (6700) and MCT detector which was cooled by liquid N_2. Firstly, a certain amount of KBr was filled into the reaction cell, and then covered with 0.2 g catalyst. The reaction cell was placed in the test chamber and heated to 175 °C under N_2 flow for 30 min to remove adsorbed impurities and then cooled to room temperature. In order to simulate the photocatalytic CO_2 reduction process, the CO_2 and H_2O were passed into the reaction cell. In this condition, a certain amount of CO_2 and H_2O could be adsorbed on the surface of sample and then purged with N_2. Subsequently, the sample was irradiated under visible light. A 300 W Xenon arc lamp was used as the light source.

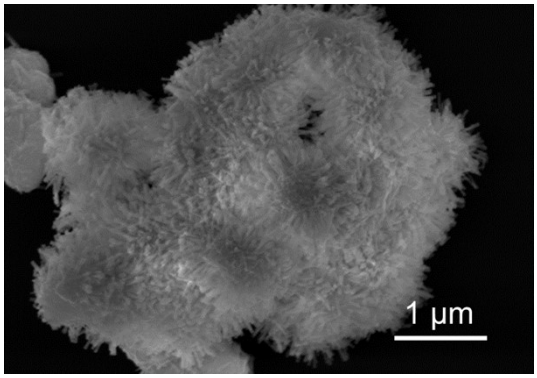

Fig. S1. TEM images of 2Mg-In_2O_3.

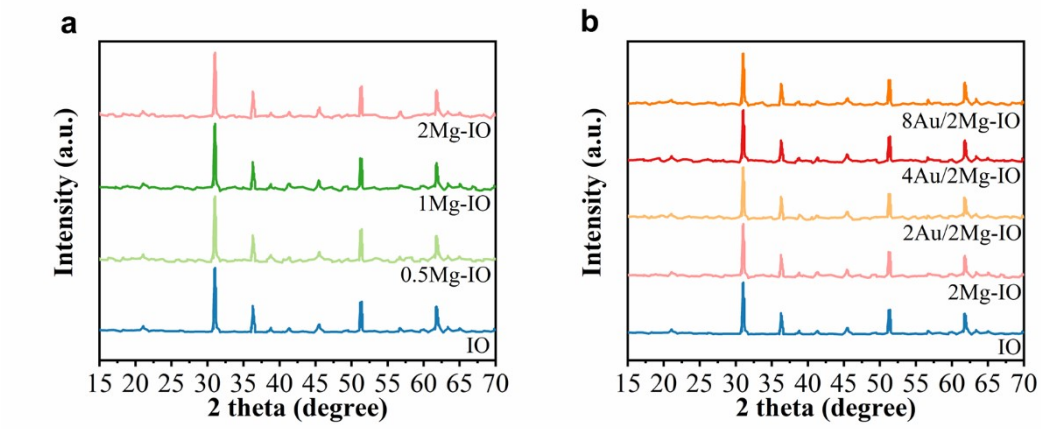

Fig. S2. XRD patterns of In_2O_3, xMg-In_2O_3 and yAu/2Mg-In_2O_3 samples.

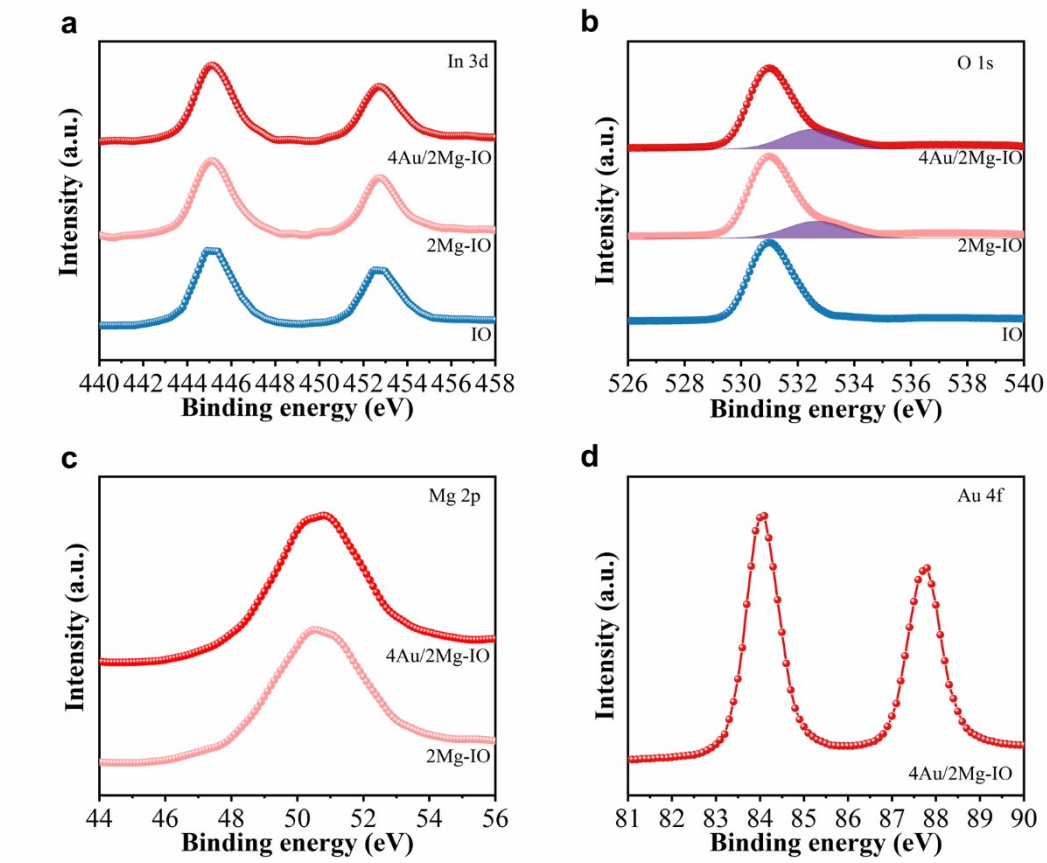

Fig. S3. (a) In 3d XPS spectra, (b) O 1s XPS spectra, (c) Mg 2p XPS spectra, and (d) Au 4f XPS spectra of In_2O_3, 2Mg-In_2O_3 and 4Au/2Mg-In_2O_3 samples.

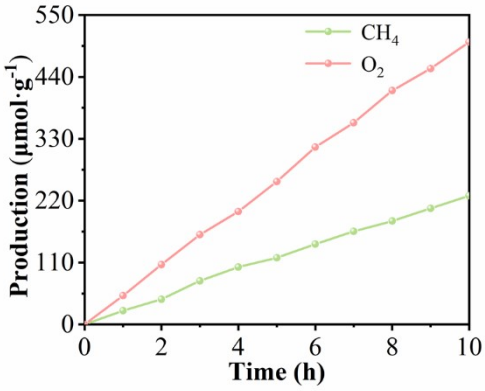

Fig. S4. Time-dependent photocatalytic O_2 and CH_4 production over 4Au/2Mg-In_2O_3 under light irradiation of 10 h.

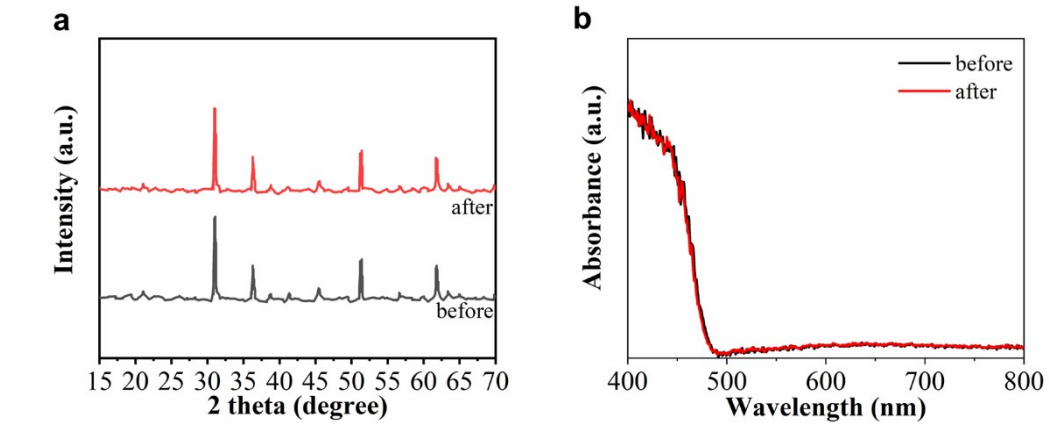

Fig. S5. (a) XRD patterns and (b) DRS spectra of 4Au/2Mg-In_2O_3 at different stages.

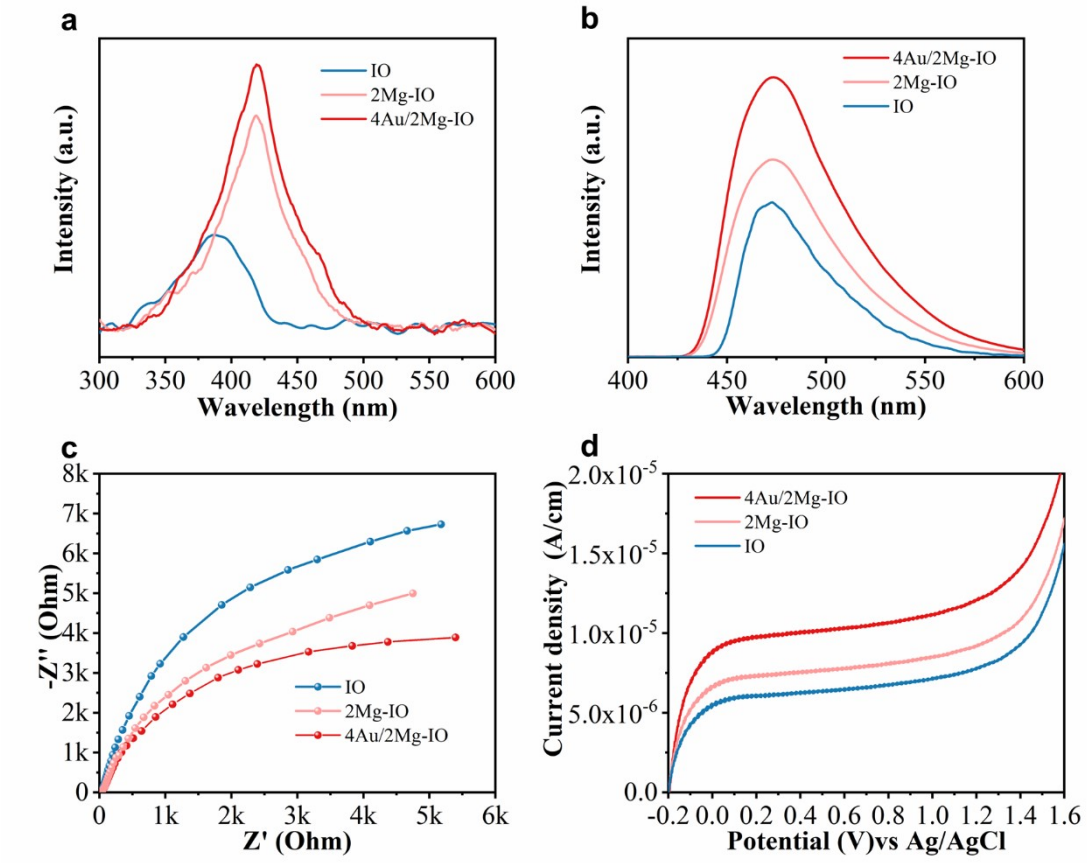

Fig. S6. (a) SS-SPS spectra, (b) Fluorescence spectra related to the formed ·OH amounts, (c) EIS spectra and (d) I–V curves under irradiation with UV–Vis light over In_2O_3, 2Mg-In_2O_3 and 4Au/2Mg-In_2O_3 samples.

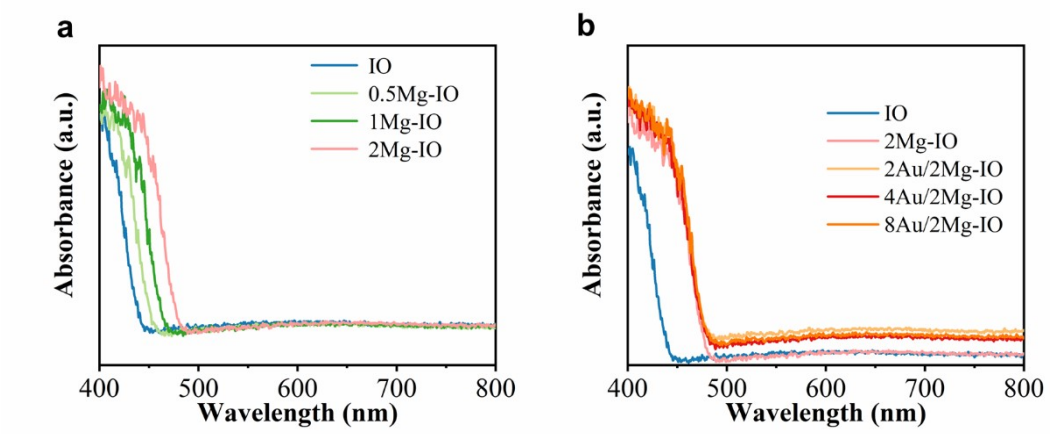

Fig. S7. DRS spectra of In_2O_3, xMg-In_2O_3 and yAu/2Mg-In_2O_3 samples.

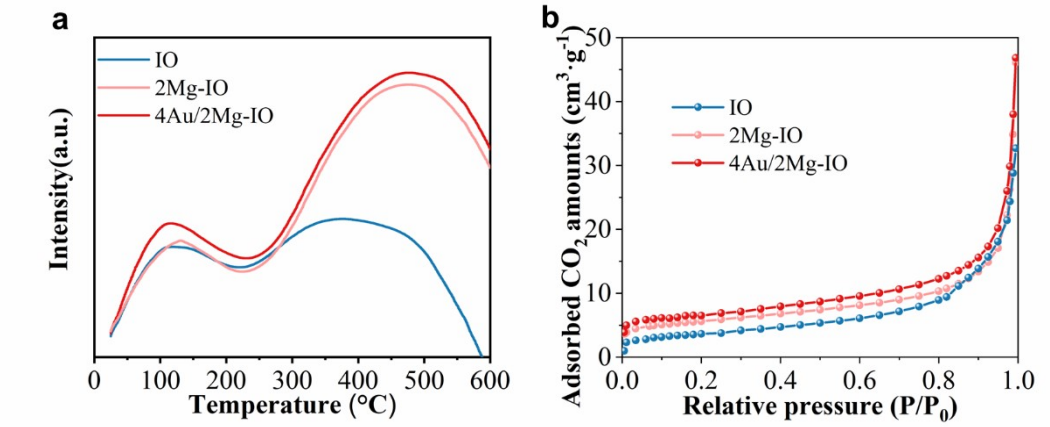

Fig. S8. (a) CO_2-TPD curves and (b) CO_2 adsorption–desorption isotherms of In_2O_3, 2Mg-In_2O_3 and 4Au/2Mg-In_2O_3 samples.

Table S1. Photocatalytic activity of CO_2 reduction conversion over different samples.

Catalyst	Rate of product (μmol/g/h)			CH_4 selectivity
	CO	CH_4	O_2	(%)
In_2O_3	15.7	2.1	12.5	11.8
0.5Mg-In_2O_3	17.3	2	13.1	10.4
1Mg-In_2O_3	1.5	9.6	20.7	86.5
2Mg-In_2O_3	0	12.7	26.2	100
2Au/2Mg-In_2O_3	0	19.2	40.1	100
4Au/2Mg-In_2O_3	0	24.5	51.2	100
8Au/2Mg-In_2O_3	0	22.1	45.3	100

Table S2. The comparison of catalytic performance with representative state-of-the-art photocatalysts for photocatalytic reduction of CO_2.

Catalysts	Production rate of CO (μmol/g/h)	Production rate of CH_4 (μmol/g/h)	References
4Au/2Mg-In_2O_3	-----	24.50	this work
In_2O_3@InP_{60}/Cu_2O-1	2.74	7.76	[S1]
20ZFO/10RGO/IO	8.85	1.95	[S2]
Cu-In_2O_3/C	43.70	15.90	[S3]
H-CeO_{2-x}@In_2O_{3-x}	9.67	1.95	[S4]
NH_2-UiO-66/Au/In_2O_3	8.56	0.19	[S5]
WO_3/In_2O_3	6.60	5.40	[S6]
In_2O_3@TiO_2-10	1.50	11.10	[S7]

Table S3. Photocatalytic activity of CO_2 reduction conversion over 4Au/2Mg-In_2O_3 for 10 h.

Time	Rate of product (μmol/g/h)			CH_4 selectivity
	CO	CH_4	O_2	(%)
1	0	24.5	51.2	100
2	0	44.8	106.4	100
3	0	77.5	159.6	100
4	0	102.0	200.7	100
5	0	118.3	253.9	100
6	0	142.9	315.3	100
7	0	165.4	358.4	100
8	0	183.7	415.6	100
9	0	206.3	454.7	100
10	0	228.8	501.9	100

Table S4. Photocatalytic activity of CO_2 reduction conversion over 4Au/2Mg-In_2O_3.

Time	Rate of product (μmol/g/h)			CH_4 selectivity
	CO	CH_4	O_2	(%)
1	0	24.5	51.2	100
2	0	25.2	51.4	100
3	0	25.4	51.8	100
4	0	24.3	50.9	100
5	0	25.2	52.1	100
6	0	24.1	51.7	100
7	0	23.9	51.3	100
8	0	25.4	50.6	100
9	0	25.3	50.9	100
10	0	24.3	51.5	100
11	0	24.1	51.9	100
12	0	24.9	50.9	100
13	0	23.8	51.7	100
14	0	25.7	51.4	100
15	0	25.2	52.5	100
16	0	25.1	50.7	100
17	0	24.6	50.1	100
18	0	23.7	50.9	100
19	0	24.3	51.5	100
20	0	24.1	51.6	100

References

[S1] Y. Wang, J. Xu, J. Wan, J. Wang, L. Wang. J. Colloid Interface Sci. 2022, 616, 532-539.

[S2] J. Li, F. Wei, C. Dong, W. Mu, X. Han. J. Mater. Chem. A. 2020, 8, 6524-6531.

[S3] A. Zhou, C. Zhao, J. Zhou, Y. Dou, J. Li, M. Wei. J. Mater. Chem. A. 2023, 11, 12950-12957.

[S4] Q. Xu, J. Jiang, X. Wang, L. Duan, H. Guo. Rare Met. 2023, 42, 1888-1898.

[S5] X. Li, C. Fang, L. Huang, J. Yu. J. Colloid Interface Sci. 2024, 655, 485-492.

[S6] Y. He, Z. Yang, J. Yu, D. Xu, C. Liu, Y. Pan, W. Macyk, F. Xu. J. Mater. Chem. A. 2023, 11, 14860-14869.

[S7] Y. Wang, W. He, J. Xiong, Z. Tang, Y. Wei, X. Wang, H. Xu, X. Zhang, Z. Zhao, J. Liu. Fuel. 2023, 331, 125719.